Journal of Asian Earth Sciences 218 (2021) 104865

Contents lists available at ScienceDirect

Journal of Asian Earth Sciences

journal homepage: www.elsevier.com/locate/jseaes

Variable vertical movements and their deformation behaviors at convergent plate suture: 14-year-long (2004–2018) repeated measurements of precise leveling around middle Longitudinal Valley in eastern Taiwan

Horng-Yue Chen [a], Jian-Cheng Lee [a,*], Hsin Tung [a], Chien-Liang Chen [b], Hung Kyu Lee [c]

[a] Institute of Earth Sciences Academia Sinica, Taiwan
[b] Central Geological Survey, MOEA, Taiwan
[c] Department of Civil Engineering, Changwon National University, South Korea

ARTICLE INFO

Keywords:
Precise leveling
Vertical movement
Longitudinal Valley fault
Plate suture
Seismic cycle
Taiwan

ABSTRACT

To better characterize the vertical movements and the deformation behaviors across the plate suture of an arc-continent collision, we conducted annual repeated measurements on two precise leveling routes in a length of 34 and 37 km, respectively, across the middle part of the Longitudinal Valley in eastern Taiwan in 2004–2018. The 14-year-long results showed that the Longitudinal Valley fault (LVF) dominates the surface deformation: a) the middle LVF (Juisui fault) exhibited partially locked in the upper few kilometers, with a cumulative uplift rate of 9–10 mm/yr in a distance of 4 km; b) the southern LVF (Chihshang fault) showed a creeping behavior with a vertical rate of 24–27 mm/yr. In addition, we are able to characterize other features, including 1) tilting upward to the west in the eastern Central Range, suggesting activity on the west-dipping Central Range fault; 2) the hanging wall of the LVF showed tilting downward behavior to the east; 3) the Chimei fault, a suspected active fault, revealed active slip on the sub-vertical fault plane, that caused a vertical rate of 8–9 mm/yr. Putting the results under global ITRF system, the whole Juisui route was moving downward, supporting the notion that NNW subduction of the Philippine Sea plate starts around the latitude of the middle of the Longitudinal Valley. Finally, the co-seismic vertical deformation of the 2013 M_L6.4 Juisui earthquake was characterized by tilting upward to the west, consistent with stick–slip on the deeper part of a west-dipping interface of the forearc basement.

1. Introduction

Over the past 40 years since early 1980s, a variety of geodetic measurements have been carried out in order to investigate surface deformation around the Longitudinal Valley in eastern Taiwan, the on-land plate suture between the converging Philippine Sea plate and Eurasia. The measurements involved different techniques, such as precise leveling (Lee and Yu, 1985; Yu and Lee, 1986; Liu and Yu, 1990; Yu et al., 1992; Yu and Chen, 1994; Lee et al., 2006; Chen et al., 2007; Chen et al., 2009; Chen et al., 2011; Chen et al., 2012; Murase et al., 2013), trilateration surveys (Lee and Yu, 1985; Yu and Lee, 1986; Liu and Yu, 1990; Yu et al., 1992; Lee and Angelier, 1993; Lee et al., 2006), Global Positioning System (GPS) measurements (Yu and Kuo, 2001; Chen et al., 2006; Lee et al., 2006; Chen et al., 2007; Chen et al., 2009; Chen et al., 2012), and Interferometry Synthetic Aperture Radar (InSAR) analyses (Hsu and Bürgmann, 2006; Yen et al., 2011; Peyret et al., 2011). The fulfilled results indeed allowed not only better locating surface traces of the major active faults but also characterizing the associated surface deformation during interseismic periods as well as a few co-seismic events, often by the aide of further kinematic or dynamic modeling (Chen et al., 2009; Huang et al., 2012; 2014; Thomas et al., 2014; Avouac, 2015; Thomas et al., 2017). Fig. 1 shows the continuous GPS station velocities around the Longitudinal Valley in 1991–2018, revealing significant horizontal velocity changes of about 30 mm/yr, characterizing by thrusting with substantial left-lateral component, across the middle and southern part of the Longitudinal Valley Fault (LVF). The 150-km-long LVF is composed of several segments with their local names, from north to south, the Lingding fault, the Fenglin fault, the Juisui fault, the Chihshang fault, and the Lichi fault. On the other hand, the GPS velocities changed the moving direction and decreased significantly with a clockwise rotation from NW to NNE in the northern part of the Coastal Range. We can also notice several moderate to large

* Corresponding author.
E-mail address: jclee@earth.sinica.edu.tw (J.-C. Lee).

https://doi.org/10.1016/j.jseaes.2021.104865
Received 3 June 2020; Received in revised form 22 January 2021; Accepted 26 January 2021
Available online 17 June 2021

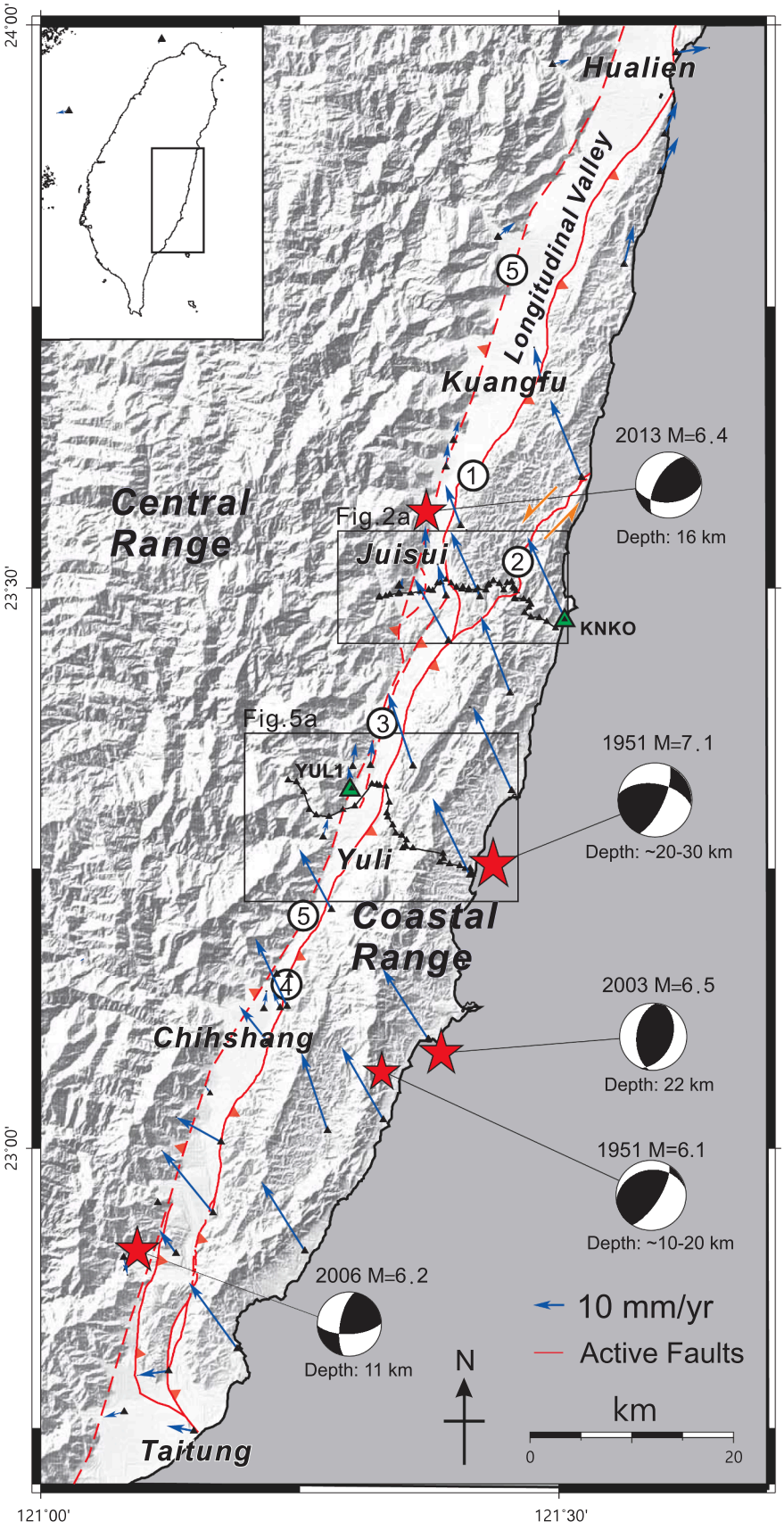

Fig. 1. GPS station velocities (1991–2018) under ITRF framework and major active faults around the Longitudinal Valley and the Coastal Range in eastern Taiwan. The GPS data show that the difference of GPS stations across the Longitudinal Valley fault is about 30 mm/yr. Historical large earthquakes located in the middle of the Longitudinal Valley are shown by red stars with focal mechanisms. In this study we conducted two leveling routes (Juisui and Yuli routes) across the middle part of the Longitudinal Valley. Red lines represent major active faults: (1) Juisui fault; (2) Chimei fault; (3) Yuli fault; (4) Chihshang fault; (5) Central Range fault. Green triangles: continuous GPS stations used for calibration into global ITRF coordinate system. (For interpretation of the references to colour in this figure legend, the reader is referred to the web version of this article.)

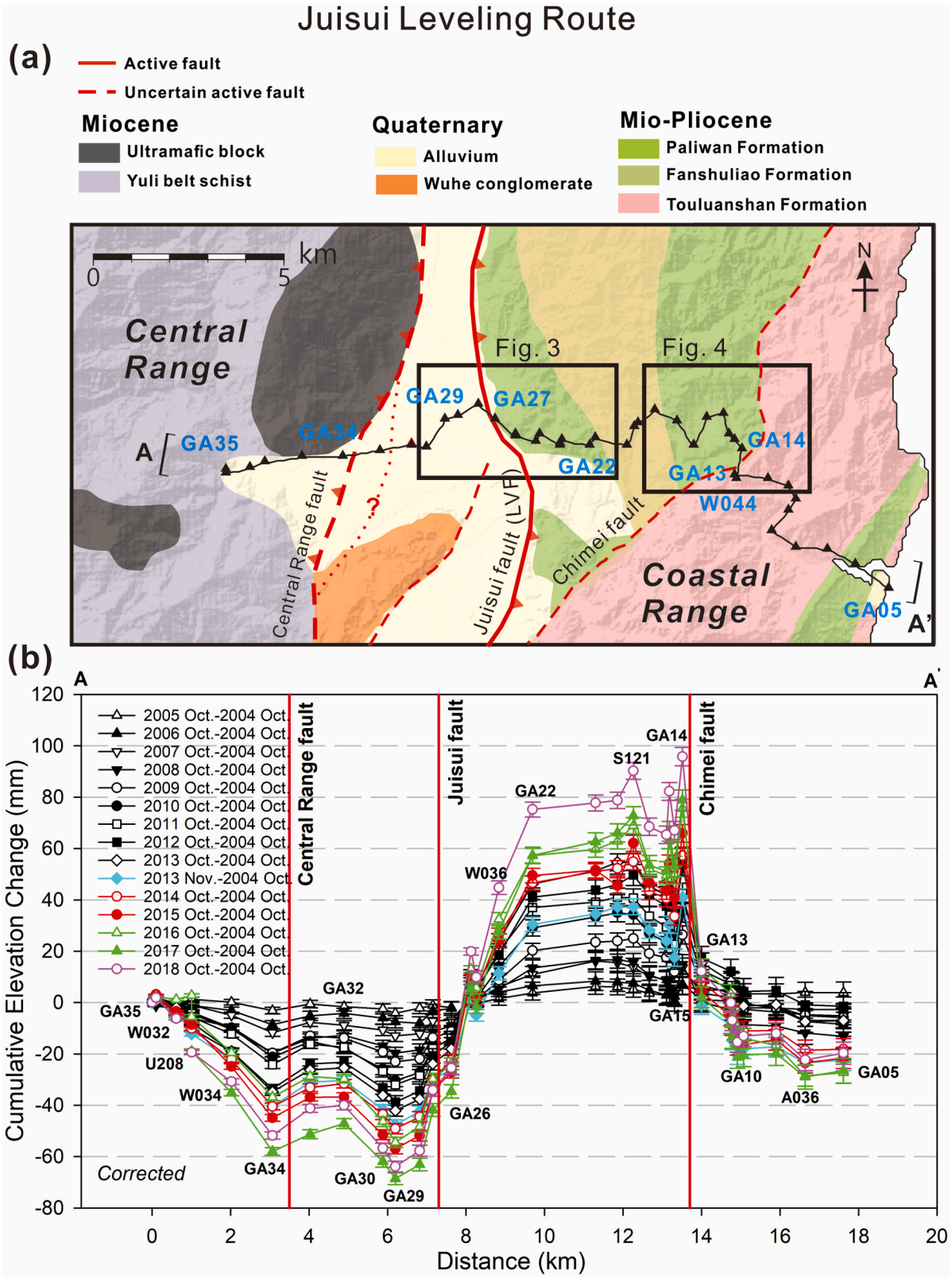

Fig. 2. Detailed distribution of the benchmarks (a) and results of cumulative elevation change from annual repeated measurements in 2004–2018 (b) in Juisui leveling route. Geological maps: after Chen and Wang (1986) for the Coastal Range and the Longitudinal Valley; after Central Geological Survey (2000) for the Central Range. The Juisui leveling route is composed of 42 benchmarks in a length of 34 km. The reference point for calculating the elevation changes was set at the westernmost benchmark, GA35. The route run across three major mapped faults, from west to east, the Central Range fault, the Juisui fault (northern LVF), and the Chimei fault. Significant elevation changes occurred across the Juisui fault as well as the Chimei fault (see detailed descriptions in the main text).

historical earthquakes had occurred quite frequently around this on-land plate suture in the past decades.

Among these geodetic approaches, it appeared that precise leveling provided one of the highest accuracy data sets for detecting and characterizing the vertical deformation, especially for near fault movements. In this study, we focused on two middle segments of the LVF, the Juisui fault and the Chihshang fault, and conducted two leveling routes, the Juisui and Yuli routes, respectively (Fig. 1), with annually repeated campaigned surveys. According to the previous GPS and leveling studies, the middle part of the LVF around the town of Yuli showed a rapid vertical motion across the fault zone with an average rate of 24 mm/yr in 1991–1999 (Yu and Kuo, 2001) and 30 mm/yr in 2008–2012 (Murase et al., 2013). Meanwhile, we found that the previous benchmarks were not long and dense enough to overly understand and pinpoint the movement behaviors along multiple fault branches (or other subsidiary faults). On the other hand, in addition to the LVF there exist other possible active faults in the surrounding areas, such as the Central Range fault, the Yuli fault, and the Chimei fault, which were not well covered by the previous shorter leveling routes. As a result, we prolonged these two pre-existing leveling routes in order to across the above-mentioned active faults from eastern Central Range to the coastline of the Coastal Range (Fig. 1). We also densified benchmarks in the near-fault zones to clarify and better characterize the deformation behaviors in the study area around the middle part of the Longitudinal Valley.

2. Benchmark implantation and data acquisition

Since the early years of 2000 s, we began to conduct annual surveys along two east–west direction leveling routes (Juisui and Yuli routes, Fig. 1) in the areas of the middle Longitudinal Valley. We adopted the benchmarks which had been implanted by different organizations, including CGS (Central Geological Survey, Ministry of Economic Affairs), IES (Institute of Earth Sciences, Academia Sinica), and MOI (Ministry of Interior). These original two routes were designed to run across and be primarily perpendicular to the NNE-SSW trending LVF, as the main known active fault in the area.

In 2004, we prolonged the Juisui route and started to conduct annual surveys. Later on, we implanted two near-fault dense arrays across the LVF (here the Juisui fault) and the Chimei fault in 2013, within the Juisui route. In 2009, we prolonged the Yuli leveling route, in order to extend eastward to across the entire Coastal Range. Furthermore, in 2010 we densified benchmarks in the near-fault zone across the LVF (here the Chihshang fault) at a spacing of every 20–40 m.

The field surveys of the leveling procedure followed the first-order class I geodetic leveling procedure (Schomaker and Berry, 1981), and adopted an even stricter requirement for double-run difference tolerances in a single section. Furthermore, a number of stringent specifications were applied to the levelling field work in order to ensure a high accuracy. In practice, the maximum permissible vertical difference in sight lengths between forward and backward sights was under 0.5 m per set-up; and the cumulative difference was limited to 1.5 m per section. The maximum length of sight was restricted to within 30 m in order to reduce the influence of atmospheric refraction. The minimum and maximum sight ground clearances (or staff readings) were 0.3 m and 2.7 m, respectively. The difference in a section of one-way length K greater than 2.5 mm* $K^{0.5}$ would be rejected, according to our field experiences under the particular atmospheric circumstance in Taiwan (Chen et al., 2012). Blunders were carefully checked during post-processing. Systematic errors, such as atmospheric refraction, rod calibration, thermal expansion, and collimation errors, etc., were carefully corrected. The cumulated error over a long distance s (a few tens of kilometers) is estimated to be about 1.0 mm* $s^{0.5}$.

Table 1
Relative velocities of Juishui leveling route from 2004 to 2018.

Years\Stations	GA35-GA34	GA29-GA22	GA14-GA10
	Vertical Velocity (mm/yr)		
2005–2004	−3.1	7.9	−3.1
2006–2004	−4.3	7.0	−5.3
2007–2004	−3.9	8.0	−5.4
2008–2004	−4.9	8.3	−6.0
2009–2004	−3.9	8.7	−5.9
2010–2004	−3.5	9.9	−6.3
2011–2004	−3.5	9.9	−6.3
2012–2004	−4.2	10.0	−6.5
2013 Oct.-2004	−3.9	9.8	−6.4
2013 Nov.-2004	−4.0	7.8	−6.1
2014–2004	−3.7	8.7	−6.3
2015–2004	−3.7	8.9	−6.9
2016–2004	−2.8	8.6	−6.6
2017–2004	−4.1	9.0	−7.2
2018–2004	−3.5	9.3	−7.4

3. Results of Juisui route

3.1. General description

The Juisui leveling route (Fig. 2) is composed of 42 benchmarks (not counting the dense benchmarks in two near-fault zones), which started from Hongyeh village in the eastern flank of the Central Range. It runs, from west to east, across the buried Central Range fault, the Juisui fault (a middle segment of LVF) and the Chimei fault to the eastern coastline with a 34 km leveling length. We conducted repeated annual surveys along this leveling route in 2004–2018. Furthermore, in order to better characterize the near fault surface deformation, we implanted two dense benchmarks arrays at the spacing of every 20–40 m for the Juisui fault and the Chimei fault in 2013. Bi-annual or annual repeated measurements were then conducted in 2013–2018.

During our survey period, on Oct. 31, 2013, a moderate earthquake of M_L 6.4 occurred with an epicenter near the foothill of Central Range about 10 km north of the Juisui leveling route with a focal depth of 15–18 km (Fig. 1). Due to the earthquake, we conducted the additional leveling measurement 2–3 weeks after the main shock in Nov. 2013. By comparing with the precedent measurement 1–2 weeks before the earthquake, we found substantial vertical coseismic motion along the Juisui route, although no surface breaks being observed. We will describe more in detail later in the section of Discussion.

Fig. 2b illustrates the cumulative vertical changes of each benchmark in Juisui route with respect to the westernmost site GA35. We compiled 15 repeated annual measurements in a 14-year time span of 2004–2018. Please note that we removed the earthquake-induced surface vertical movements due to 2013 earthquake, in order to better illustrate the secular, interseismic surface vertical velocities.

3.2. Activity on the Central Range fault?

In Fig. 2b, we can find that slight but clear gradual westward uplift occurred in the eastern side of Central Range with a steadily rate of 3.2–4.1 mm/yr, compared to the benchmarks in the Longitudinal Valley. There is a velocity gradient break around the mountain foot of the Central Range against the valley (between sites GA34 and GA33), where coincides with the expected surface projection of the Central Range fault (Fig. 2a). As a consequence, it implies continuous activity of the buried Central Range fault, albeit without evidence of surface creep, at least in this 14-year-long time span. Although the exact location of surface trace of the fault remains questionable, we attributed it to be approximately along the edge of hills near GA34. Different fault types for the Central Range fault have previously been proposed, as either a major thrust or normal fault, in the past decades, and still under debate (Biq, 1972; Crespi et al., 1996; Shyu et al., 2005; Chen et al., 2009). Here our 14-

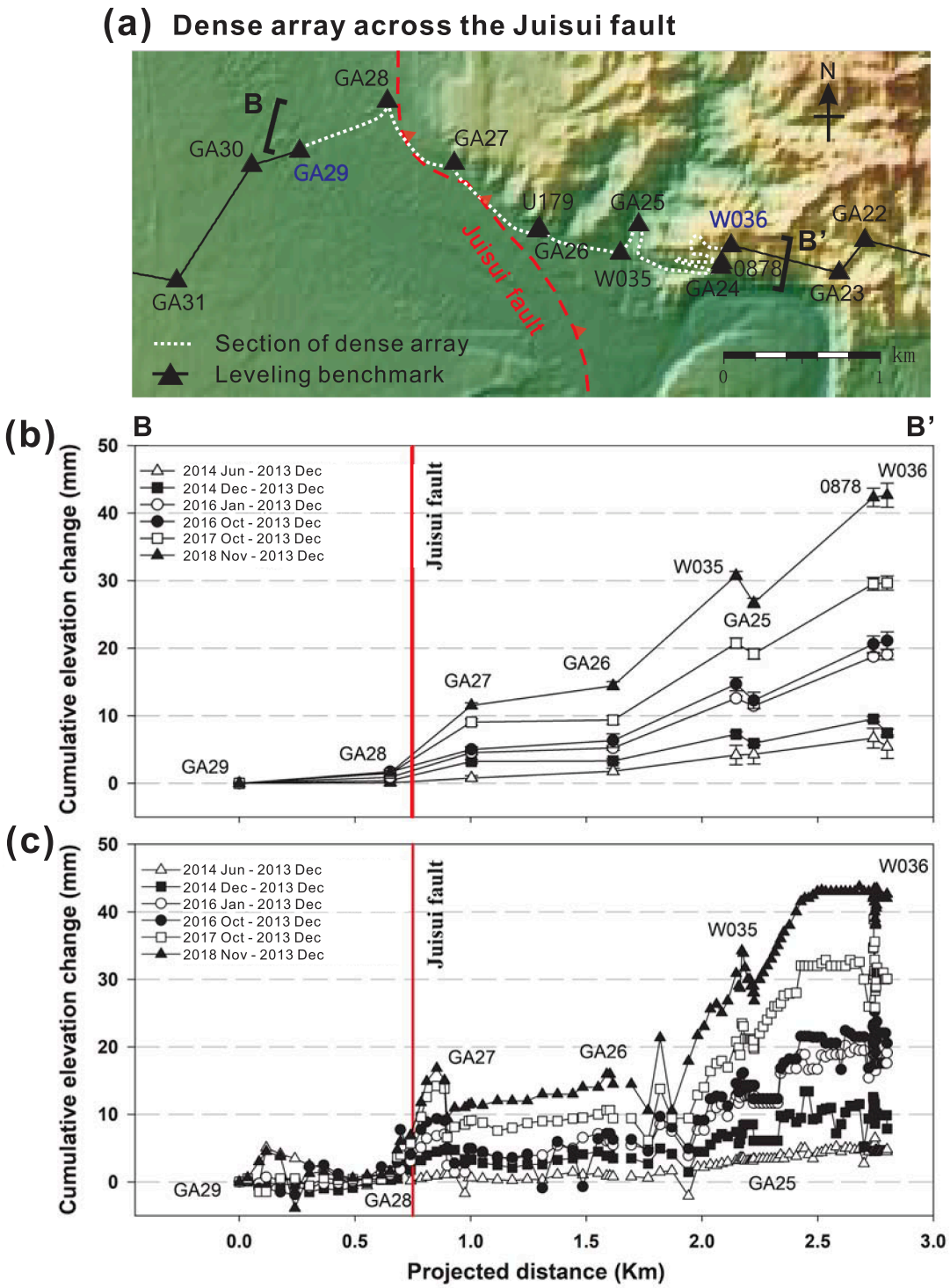

Fig. 3. Results of near-fault leveling observations across the Juisui fault. (a) Map of distribution of the densified benchmarks at a spacing of 30–40 m across the fault from GA29 to W036. (b) Results of elevation changes on the original benchmarks in 2013–2018. (c) Results of elevation changes on the densified benchmarks in 2013–2018. The surface trace of the Juisui fault is located just east of GA28 and closely follows the geomorphic scarp until GA26. Note that some artifacts appeared in the profile curves might be attributed to the obliquity between the orientation of the profiles and the change of the fault trend.

year-long leveling results favor a thrust fault, coupled with a west-dipping fault plane (Fig. 2b, Table 1). In this case, our leveling results would suggest deeper slip on the fault with shallow lock, based on the tilting curve upward to the west in eastern Central Range (Fig. 2b), coupled with elastic dislocation theory (e.g., Thatcher and Rundle, 1979; Vergne et al., 2001). More rigorous modeling work is still needed, however, beyond this study.

Within the Longitudinal Valley, the vertical deformation was not substantial, however, a minor bulge occurred across the 3–5-km-wide valley (between benchmarks GA34 and GA29 in Fig. 2b). Tentatively, we interpret it to be associated with a west-dipping thrust that breaks up to the surface between GA32 and GA31. If so, whether this west-dipping thrust represents a branch of the Central Range fault remains to be determined. However, a western branch of the east-dipping LVF remains

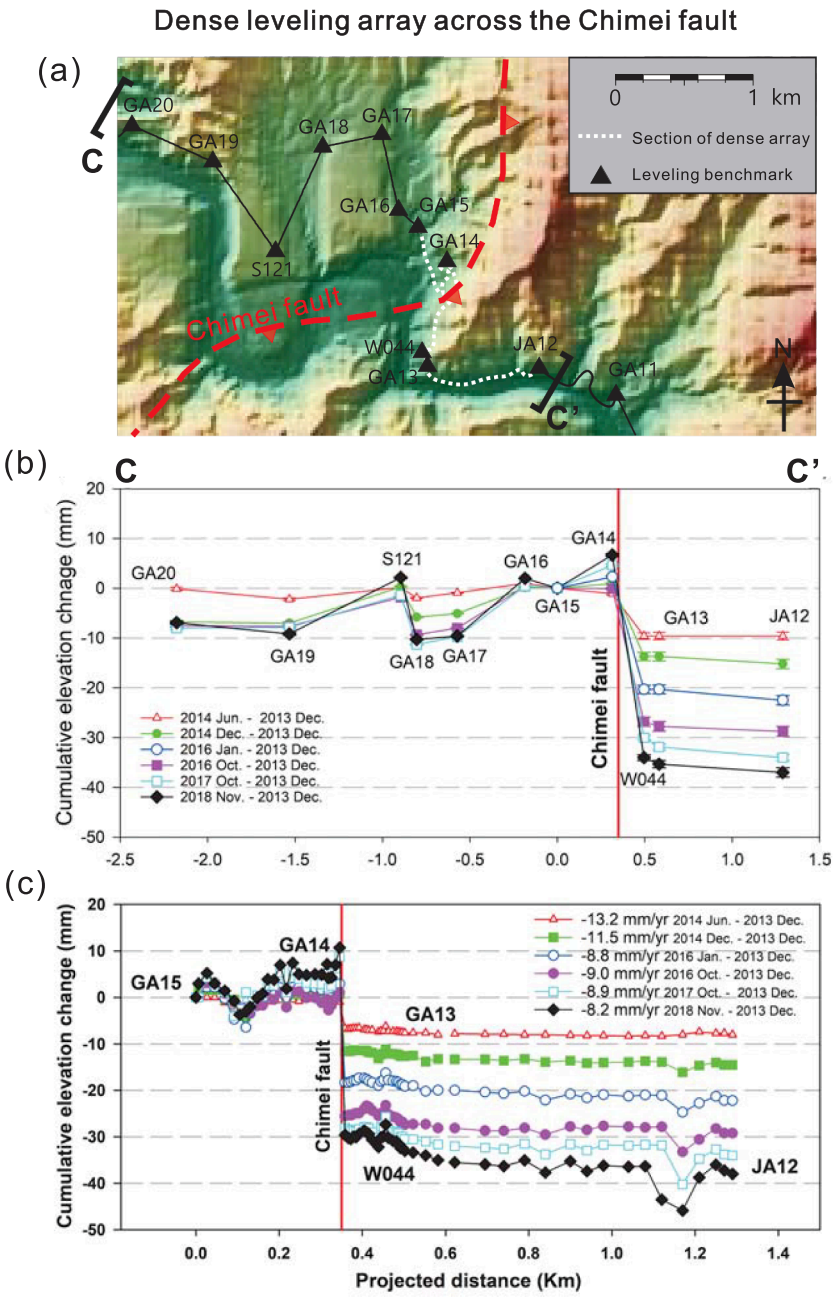

Fig. 4. Results of near-fault dense leveling array across the Chimei fault along the Juisui route. (a) Map of distribution of the densified benchmarks at a spacing of 30–40 m across the fault from GA15 to JA12. (b) Results of elevation changes on the original benchmarks in 2013–2018. (c) Results of elevation changes on the densified benchmarks in 2013–2018, indicate that uplift and subsidence are relative to GA15 station motion, used as a zero reference. Note that one needs to be careful on interpreting some stations due to their relative distance to the fault and the obliquity of the orientation of the profile to the fault trend; e.g., S121 is located much closer to the fault compared to its neighbor benchmarks. See more details in main text.

possible to produce this fold bulge. Alternatively, groundwater effects might influence the elevation changes of the benchmarks in the alluvial deposits.

3.3. The Juisui fault (LVF)

Not surprisingly, the most dramatic vertical changes for the entire leveling route occurred across the Juisui fault (Fig. 2b), one of the segments of the LVF. The cumulative vertical change was up to 135–140 mm across the Juisui fault between GA29 and GA22 in 14 years of 2004–2018, that is an average vertical rate of approximately 10 mm/yr. This is a curve of gradual increase, characterizing the cumulative vertical change in a distance of about 4 km across the fault (~1 km in footwall and ~ 3 km in hanging wall). Based on elastic dislocation theory (e.g., Thatcher and Rundle, 1979; Vergne et al., 2001), the gradually uplift in the hanging wall of a thrust during the interseismic period implies a locked or partially locked segment of the Juisui fault at the shallow few kilometers with continuous slip on the deeper part of the fault. Considering an east-dipping thrust, it would yield anticlinal folding or tilting in the hanging wall of the fault.

On the surface, the geomorphic expression associated with the Juisui fault is substantially manifested: a topographic break closely follows the foot of the Coastal Range. In more detail, the surface trace of the Juisui fault appears to be between two benchmarks: GA28 and GA27 (Fig. 3b). In 2013, we implanted a dense array of additional benchmarks at a spacing of 35–45 m between GA29 and W036 of a total number of 150 benchmarks and 5.1 km in length (Fig. 3). Our 5-year annual repeated surveys of the near-fault dense array in 2013–2018 (Fig. 3c) indicate a major fault strand is located just a few meters east of GA28; and the surface trace bends and mainly is sub-parallel to the densified leveling route from GA28 to GA26. We also noticed a few interesting small bumps around GA29 and GA27 that deserves to be further investigated in the future, although we tend to consider it to be local human construction effects.

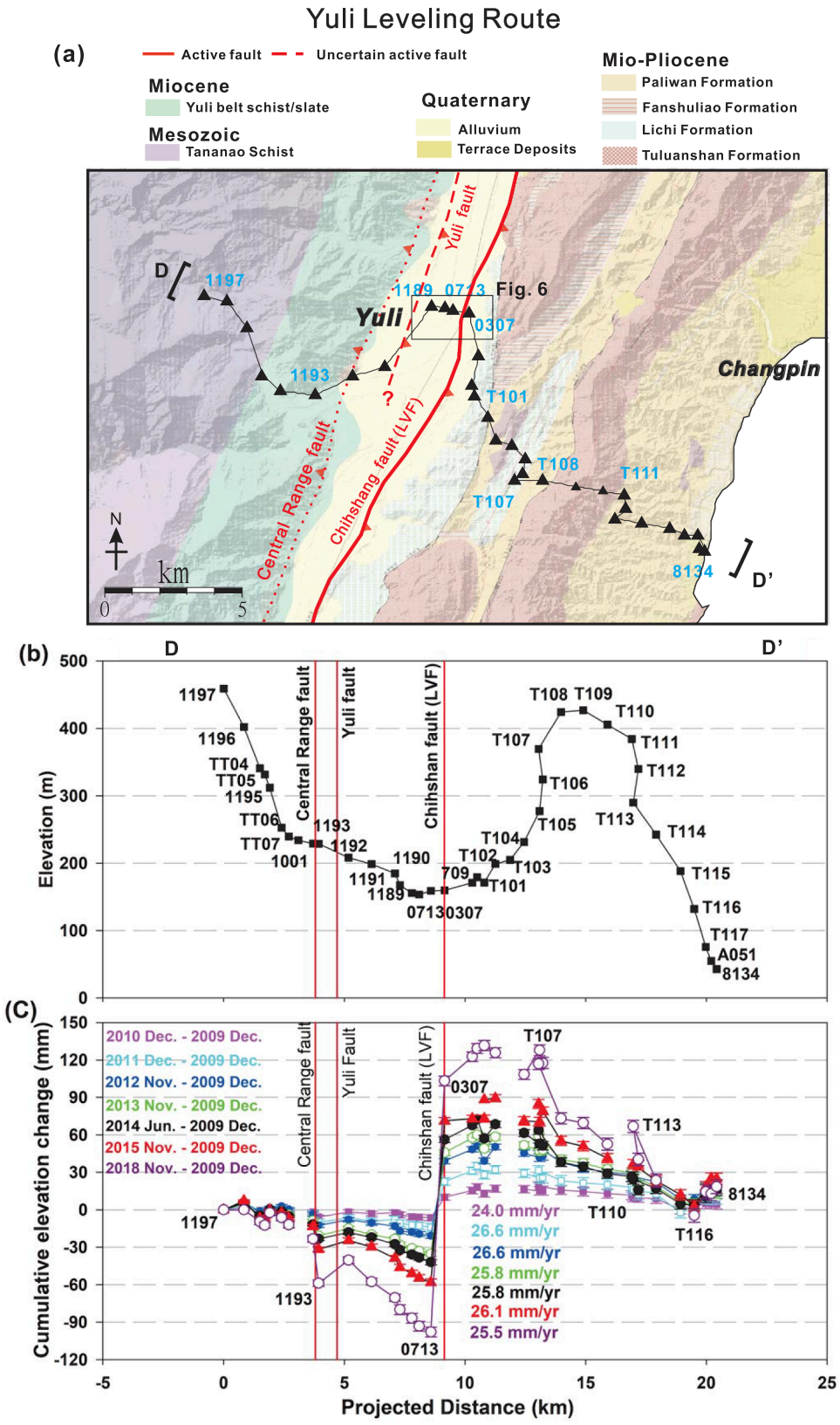

Fig. 5. Results of the Yuli leveling route. (a) Map of distribution of the benchmarks along the Yuli route. (b) Elevation profile of the Yuli route. (c) Results of cumulative elevation changes from annual repeated measurements in 2009–2018. Geological maps: after Chen and Wang (1986) for the Coastal Range and the Longitudinal Valley; after Central Geological Survey (2000) for the Central Range. Three major geological faults, crossing the leveling route, have been mapped: from west to east, the Central Range fault, the Yuli fault, and the Chihshang fault (the southern LVF). We can observe a sharp elevation change at a rate of 24–27 mm/yr across the LVF with almost symmetric tilting on both sides of the fault. Within the valley, it shows a bulge in Fig. 5c. See more explanations in the main text.

3.4. The Chimei fault

In the hanging wall of the Juisui fault within the Coastal Range, from benchmark GA22 toward the east (Fig. 2b), there was no significant vertical movement until the route encounters the Chimei fault where a sudden vertical offset occurred and coupled with a pair of drop and jump (from S121 to GA14 in Fig. 2b), then deep drop across the fault (from GA14 to GA13). We also implanted and conducted a dense array of leveling near the Chimei fault from GA15 to JA12 in 2013–2018 (Fig. 4). In Fig. 4, we can observe a slight uplift at a rate up to 3–4 mm/yr

Table 2
Relative velocities of Yuli leveling route from 2009 to 2018.

Years\Stations	1197–0713	0713–0307	0307–8134
	Vertical Velocity (mm/yr)		
2010–2009	−7.1	24.0	−12.2
2011–2009	−8.6	26.6	−13.1
2012–2009	−8.1	26.6	−12.7
2013–2009	−10.0	25.8	−13.4
2014–2009	−8.9	25.8	−12.2
2015–2009	−10.1	26.1	−11.7
2018–2009	−10.9	25.5	−12.6

occurred in Takangkou turbidite formation (also called Paliwan formation) on the NW side at a distance of about 1 km to the fault (from GA18 or GA17 to GA14 in Fig. 4). Note that the benchmark S121 is located relatively close to the fault (see Fig. 4a), compared to its neighboring ones (GA19 and GA18). Then dramatic subsidence occurred on the SE side as the route passing the Chimei fault from turbidite into andesite, at a rate of 8–9 mm/yr (Fig. 4c).

At first glance, it is not straightforward for interpreting the leveling data in terms of slip behavior of the Chimei fault. Geological deformation structures around the Chimei fault indicate that significant contraction and lateral shearing had been occurred in accompany with the faulting during geological time, such as intensive folding and strong shearing and foliation in the turbidite sequence layers on the NW side (Kuo, 2014; Chu, 2016) and abundant brittle fractures, such as numerous sets of slickenside, in the andesitic rocks on the SE side. Published regional 1:100,000 geological map (Chen and Wang, 1996) interpreted the Tuluanshan andesitic Formation thrusted over the Paliwan turbitite sequence along the Chimei fault. However, field observations from the slip kinematics data showed prevailed left-lateral oblique faulting on a nearly vertical major fault plane (Lee et al., personal communication). Keeping the geological information in mind, the leveling measurements across the Chimei fault indeed show that the Paliwan turbidite sequence is going up (with half-syncline folding) with respect to the Tuluanshan andesitic formation. Taking a sub-vertical fault plane into account, our leveling data also indicate a surface vertical creeping rate around 8–9 mm/yr along the Chimei fault. Our leveling measurements did not provide any direct data for horizontal displacement, however, data from GPS stations indicate a dominant left-lateral horizontal movement across the fault at the rate of 4–5 mm/yr (unpublished data).

3.5. Summary of the Juisui route

In summary for the Juisui leveling route, it appears that the most substantial surface vertical deformation corresponded to the activity on three previously mapped geological faults, including the Central Range fault, the Juisui fault and the Chimei fault, although the Central Range fault was widely considered a blind fault. We tentatively infer that 1) the

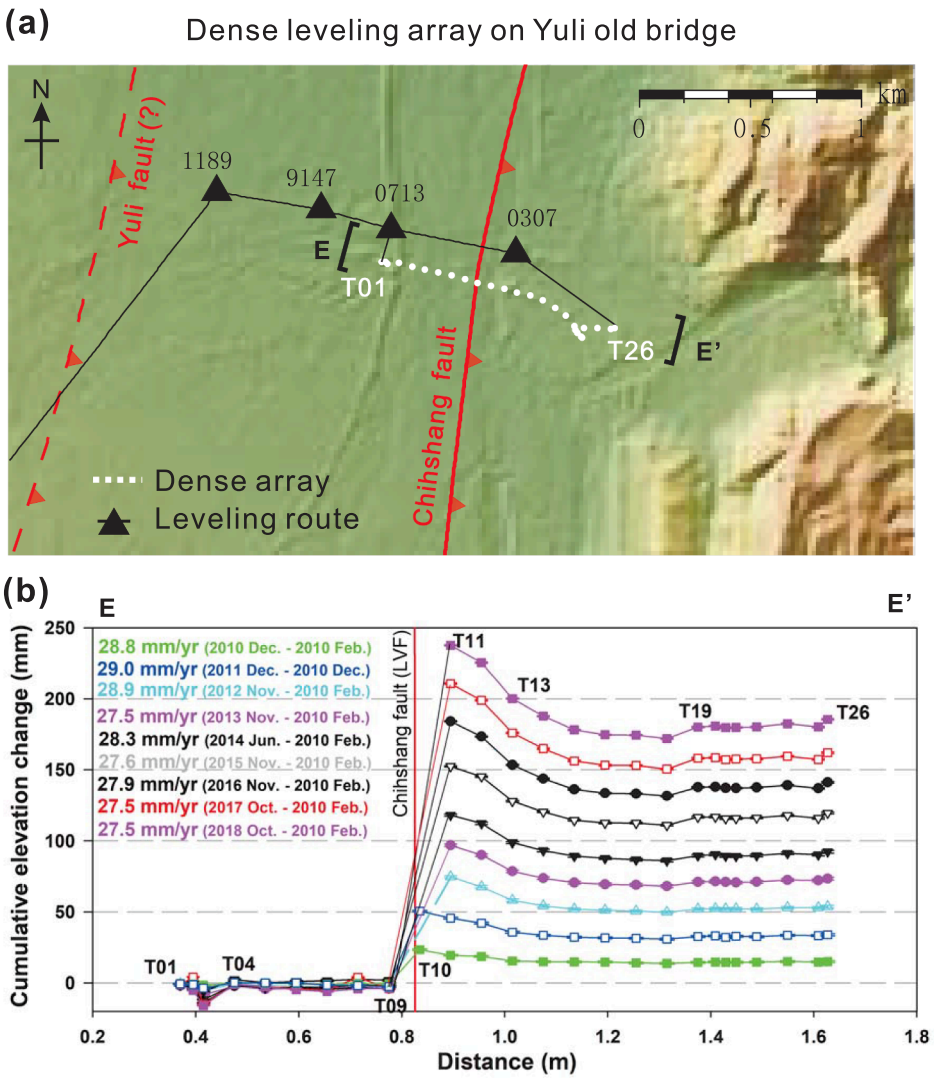

Fig. 6. Results of near-fault dense leveling array across the LVF along the Yuli route. (a) Map of the densified benchmarks at a spacing of 30–50 m across the fault from T01 to T26 in a distance of 1.2 km. (b) Results of cumulative elevation changes from annual repeated measurements in 2010–2018. The elevation change occurred in a very narrow zone between T09 and T10, with a vertical creeping rate of 27–29 mm/yr. Note that the dots in the dense array (Fig. 6a) do not represent the exact locations of the survey points.

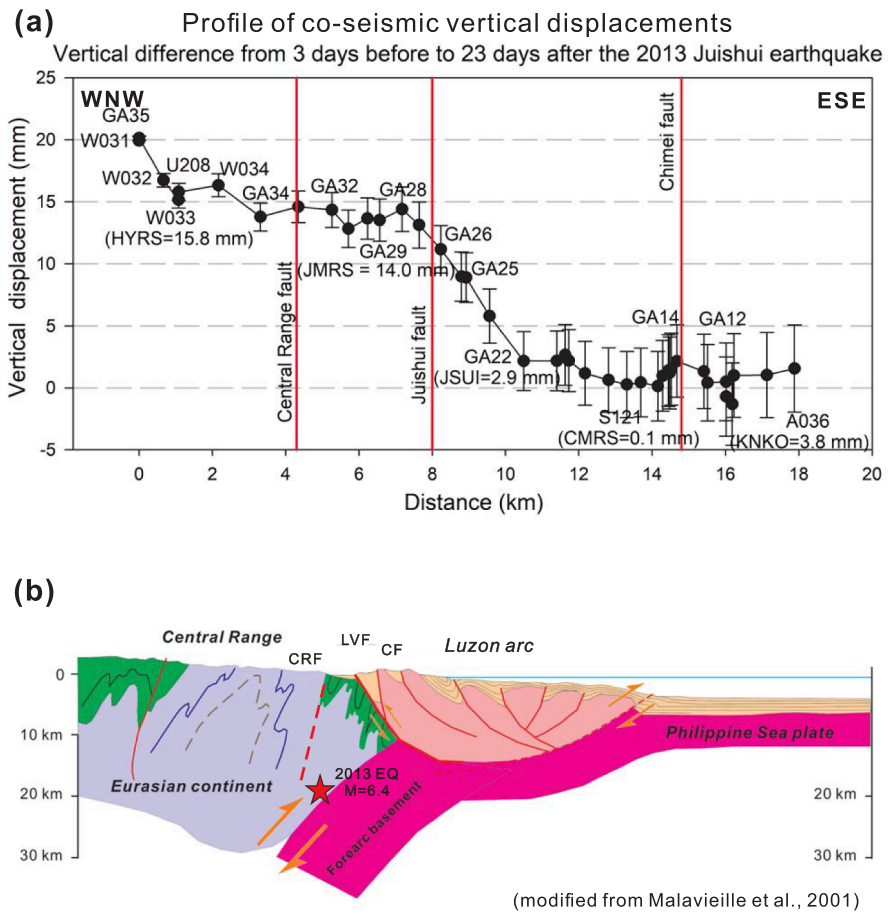

Fig. 7. (a) Vertical coseismic displacements profile along the Juisui route associated with the 2013 M_L 6.4 Juisui earthquake. (b) Geological cross section (modified from Malavieille et al., 2002) with the interpreted location of the main shock of the 2013 Juisui earthquake. CRF: Central Range fault; LVF: Longitudinal Valley fault; CF: Chimei fault. We compared the surveys before (3–10 days before) and after (18–23 days after) the Juisui earthquake to obtain the coseismic movements. The curve shows a tilting behavior upward to the west with the easternmost benchmarks stayed unmoved, implying a blind deep slip on a west-dipping structure underneath the leveling route. See main text for detailed explanations.

W-dipping Central Range fault reveals slip at depth that induced tilting upward to the west and/or folding at the shallow level in the eastern flank of the range, 2) across the Juisui fault it shows gradual uplift with a cumulative vertical rate of approximately 10 mm/yr in a distance of about 4 km, suggesting a partially locked behavior at the upper few kilometers, and 3) across the Chimei fault it exhibits uplift on the NW side (turbidite sequence) and subsidence on the SE side (massive andesite), with deformation accommodated by a sharp surface vertical creep of 8–9 mm/yr along the nearly vertical fault and a half-synclinal folding in a distance of about 1 km on the NW side turbidite.

4. Results of Yuli route

The Yuli leveling route starts from benchmark 1197 near the Nan'an waterfall in eastern Central Range and it goes across the Longitudinal Valley and the entire Coastal Range with a total length of 37 km (Fig. 5). In this section, we present results of repeated annual measurements for a 9-year time span in 2009–2018 (Fig. 5c, Table 2).

4.1. The Chihshang fault (LVF)

Fig. 5 illustrates the leveling results of the Yuli route. The cumulative elevation changes (Fig. 5c) showed a typical curve of creeping thrust faulting. It is characterized by 1) a gradual subsidence toward the Chihshang fault (a southern segment of LVF) in the footwall (western side) with a subsidence rate of 7–10 mm/yr, 2) a sharp vertical offset with a rather steady rate of 24–27 mm/yr across the fault zone, and 3) a gradual decrease of uplift in the hanging wall (eastern side) with a decreasing rate of 11–13 mm/yr.

We zoom into the near fault zone around the Chihshang fault. Similar as we did for the Juisui route, we implanted dense leveling array with benchmarks at every 30–50 m, in order to evaluate the near fault vertical movements in more details. We implanted new benchmarks on the concrete pavement of an abandoned railroad bridge (now became a bicycle tourist route), which straddles across the Chihshang fault. This is a relatively short leveling route of about 1 km long with 26 benchmarks (T01-T26) (Fig. 6). Nine repeated leveling measurements on a nearly annual basis have been conducted from 2010 to 2018. The results indicated that the Chihshang fault indeed exhibited rapid near-surface creeping, with a peak uplift rate of 27–29 mm/yr near the fault tip (between T09-T11, T10 was lost in 2011–2012, Fig. 6b). Observing the sharply tilting curves in the hanging wall, we also are wondering local block rotations and/or brittle behaviors might occur on the concrete bridge around the immediate hanging wall of the fault.

It is worth noting that the rapid creep at the shallow level on the Chihshang fault has been previously documented around the southern part of the Chihshang fault, near the town of Chihshang, about 20–30 km south of the Yuli leveling route (e.g., Angelier et al., 1997; Lee et al., 2003; Chang et al., 2009; Thomas et al., 2017). Surface creep has led to growth of fractures on numerous human constructions along the Chihshang fault, in particular in its southern part (Angelier et al., 1997; Lee et al., 2003; 2006). Our leveling results indicate that the surface rapid creep occurs not only in the southern part but also in the norther part, probably throughout the entire Chihshang fault.

Back to a broader regional scale, as mentioned above we can find the apparent tilting pattern on hanging-wall sides of the Chihshang fault (Fig. 5c). Across the entire Coastal Range of 15–20 km wide, our leveling results showed eastward tilting with a gradual subsidence rate up to

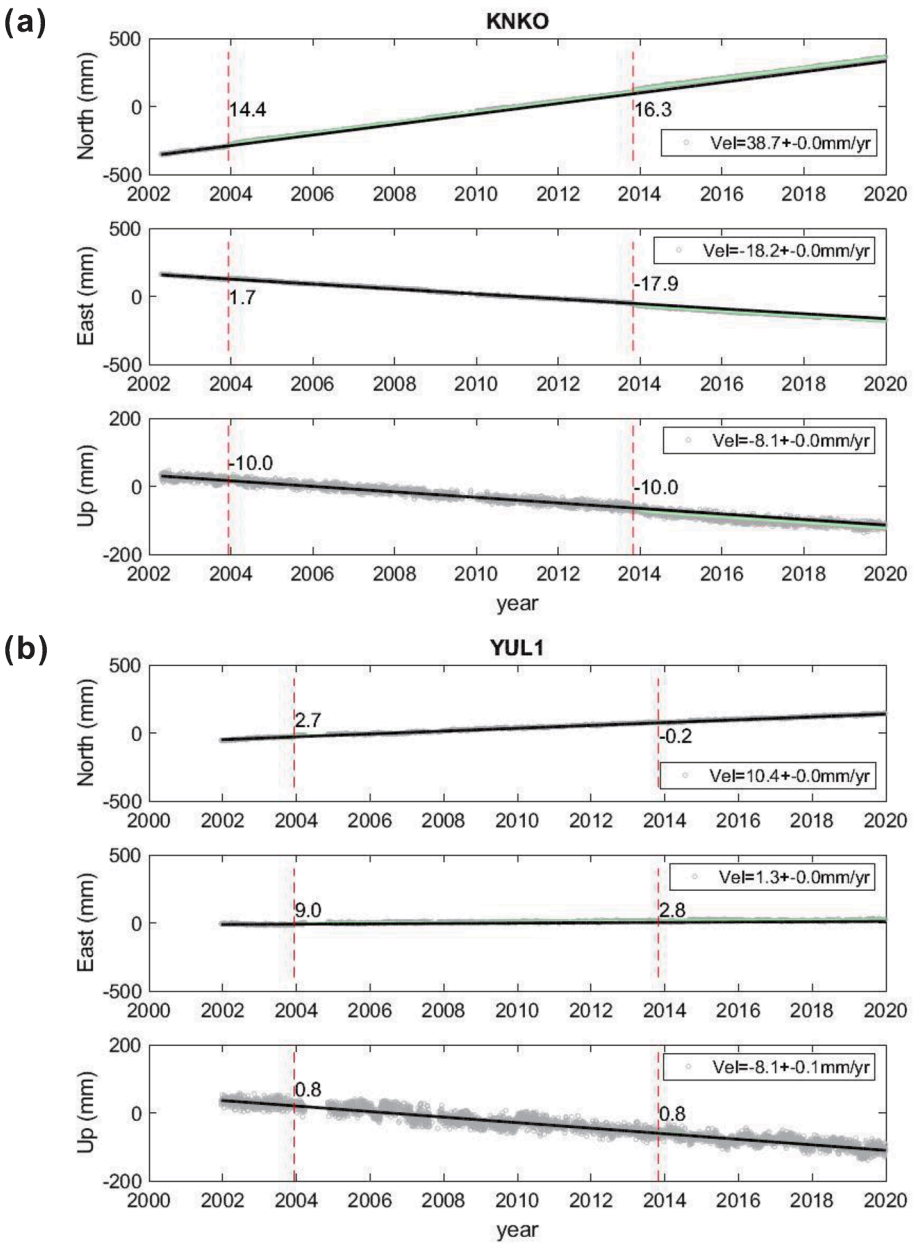

Fig. 8. Time series data illustrating the estimates of the secular velocities at two continuous GPS stations, KNKO (a) and YUL1 (b). Several moderate to large earthquakes produced coseismic vertical movements during the observation period in 2002–2012. We thus removed these coseismic effects to obtain vertical secular velocities under global ITRF coordinate system.

11–13 mm/yr in the years of 2009–2018. On top of this tilting downward to the east, we can also observe a pair of anticline and synclinal folding, between 0307 and T107, in the hanging wall of the Chihshang fault in a distance of about 5 km, indicating internal deformation within the Coastal Range.

4.2. The Central Range fault and the Yuli fault

Near the western edge of the Longitudinal Valley, the cumulative elevation changes showed a bulge shaped curve (Fig. 5c), which cut across by an east-titling curve on the eastern flank of the Central Range. The intersection of the two types of curves is located roughly on the surface projection of the Central Range fault and the surface ruptures of the 1951 M7.1 earthquake, which has previously named the Yuli fault by Hsu (1962), after his filed survey following the 1951 earthquake. Our results imply possible slight thrust slip on the presumably east-dipping Yuli fault. On the other hand, the steady east-tilting trend of vertical movement in the eastern flank of the Central Range is consistent with slip on the west-dipping Central Range fault (Fig. 5), which might juxtapose with the Yuli fault near the foot of the Central Range. However, it requires further work to clarify.

5. Discussions

5.1. The 2013 M = 6.4 Juisui earthquake

As mentioned above, the 2013 M_L 6.4 Juisui earthquake occurred in the vicinity of the Juisui leveling route (see location in Fig. 1), a few days after we just finished our annual survey. We promptly conducted an 'emergency' survey two weeks after the earthquake. By comparing the surveys before (3–10 days before) and after (18–23 days after) the 2013 Juisui earthquake we obtain the 'coseismic' vertical displacements.

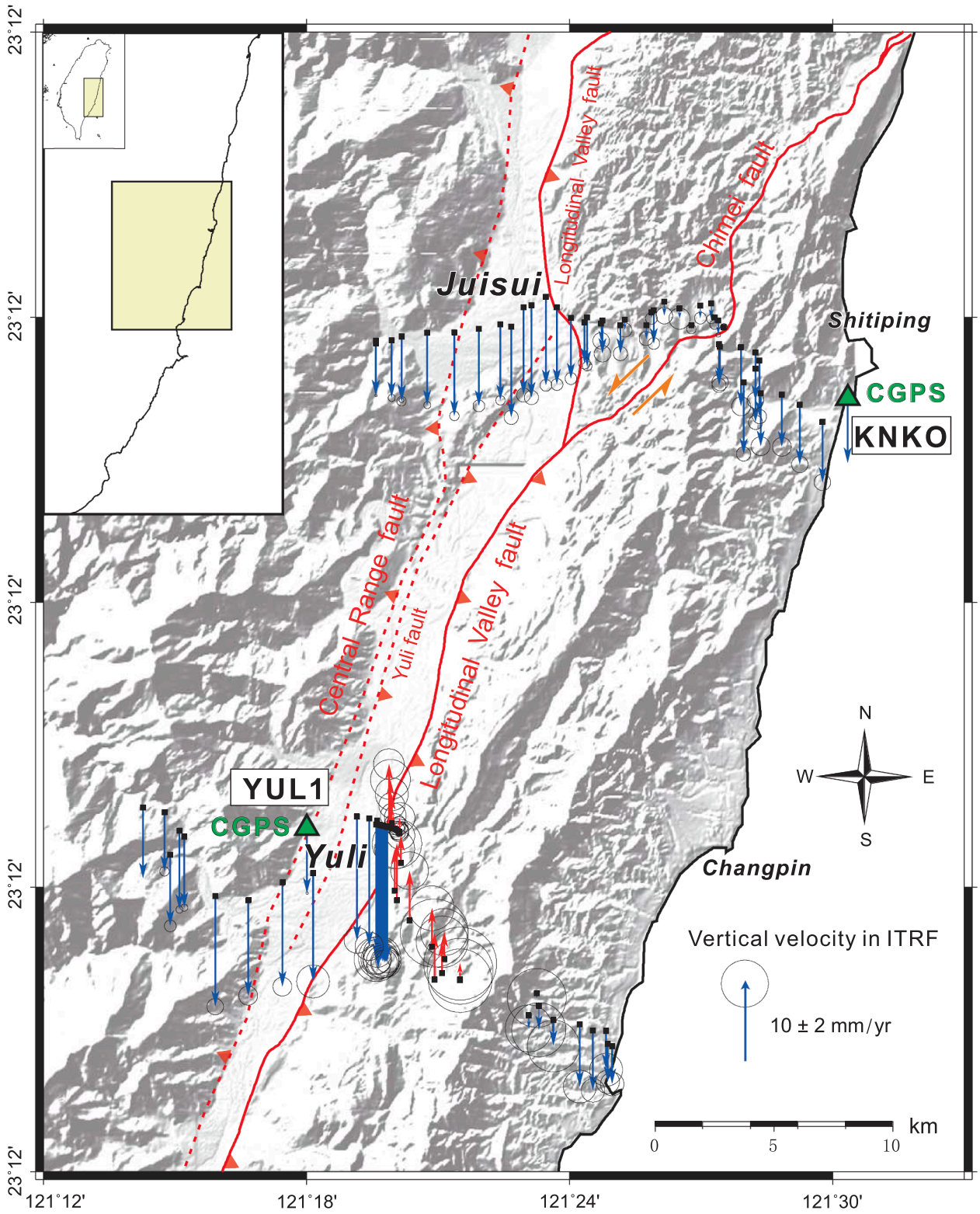

Fig. 9. Vertical secular velocity field for the two leveling routes in the middle of the Longitudinal Valley and the Coastal Range. The velocities were calibrated into global ITRF coordinate system by incorporating the two nearby continuous GPS stations, KNKO and YUL1, with the long-term time-series data. Note that the error circles represent the standard errors of the average annual velocities calculated from leveling data. Unlike obvious uplift in the hanging wall of the southern LVF in the Yuli route, the entire Juisui route is experiencing subsidence although thrust slip occurred on the LVF and the Chimei fault. This supports that the northern Coastal Range and the underlying Philippine Sea plate is undergoing subduction at the latitude of the Juisui route. See detailed descriptions in main text.

Table 3
Secular velocities of the Juisui and Yuli leveling routes under ITRF. Juishui route.

Stations	Velocity (mm/yr)	Locations	Stations	Velocity (mm/yr)	Locations
GA35	−7.0 ± 0.0	Central	GA27	−9.8 ± 0.5	Juishui
W031	−6.6 ± 0.1	Range	GA26	−7.7 ± 0.5	fault
W032	−7.3 ± 0.3	Fault	W035	−5.2 ± 0.5	
U028	−8.1 ± 0.2		GA25	−6.2 ± 0.4	
W033	−8.2 ± 0.4		GA24	−2.2 ± 0.7	
W034	−9.2 ± 0.3		W036	−4.2 ± 0.7	
GA34	−10.6 ± 0.4		GA23	−3.6 ± 0.6	
GA33	−9.8 ± 0.5		GA22	−1.3 ± 0.6	
GA32	−9.6 ± 0.4	Longitude	W038	−1.7 ± 0.6	
GA31	−11.5 ± 0.6	Valley	W039	−0.8 ± 0.5	
GA30	−11.1 ± 0.6		GA21	−4.2 ± 0.5	
GA29	−11.7 ± 0.6		GA20	−1.8 ± 0.7	
GA28	−11.2 ± 0.5		GA19	−1.3 ± 0.9	
			W041	−2.7 ± 0.0	
			S121	−0.5 ± 0.4	
			GA18	−1.6 ± 0.5	
			GA17	−2.0 ± 0.4	
			GA16	−0.9 ± 0.4	
			GA15	−1.8 ± 0.2	
			GA14	0.0 ± 0.3	
			W044	−4.5 ± 0.7	Chimei
			GA13	−5.2 ± 0.6	fault
			GA12	−7.5 ± 0.8	
			GA08	−9.1 ± 0.6	
			GA11	−6.1 ± 0.7	
			GA09	−6.8 ± 0.6	
			GA10	−7.1 ± 0.6	
			GA07	−6.7 ± 0.8	
			GA06	−6.6 ± 0.8	
			A036	−7.6 ± 0.7	
			A037	−7.2 ± 0.9	
			GA05	−7.7 ± 0.7	

Stations	Velocity (mm/yr)	Locations	Stations	Velocity (mm/yr)	Locations
I197	−9.0±0.0	Central	O307	2.3±1.1	Chihshang
I196	−7.5±0.4	Range	7O9	5.3±1.7	fault
TT04	−9.8±0.3	fault	T101	7.2±2.1	
TT05	−10.0±0.3		9148	3.5±1.2	
I195	−9.0±0.3		T102	6.3±1.6	
TT06	−9.0±0.5		T104	4.9±1.9	
TT07	−9.7±0.5		T107	5.9±2.9	
I001	−10.9±0.4		T105	3.5±2.0	
I193	−14.0±0.7		T106	4.0±2.2	
I192	−12.1±0.8	Yuli fault	T108	2.1±3.1	
I191	−13.2±0.8		T109	1.1±2.8	
I190	−13.7±1.4		T110	−0.1±2.7	
T118	−14.9±1.3		T113	−1.6±2.0	
I189	−15.7±1.1		T111	−0.6±2.5	
9147	−16.2±1.2		T112	−3.0±2.3	
0713	−16.8±1.2		T114	−3.3±2.2	
			T115	−7.9±1.4	
			T116	−7.6±1.0	
			T117	−4.9±1.4	
			A051	−4.8±1.0	
			8134	−4.8±1.0	

Meanwhile, there exit 5 GPS continuously operating reference stations (CORS), HYRS, JMRS, JSUI, CMRS and KNKO, close to the Juisui leveling route (from GPSLAB of Academia Sinica, http://gps.earth.sinica.edu.tw/). We thus used continuous GPS vertical displacements to constrain the leveling measurements and incorporated the results into the same global reference frame (Fig. 7).

In Fig. 7, we can observe the curve of the calibrated vertical coseismic displacements exhibits a general pattern of tilting upward to the west. Whereas the easternmost benchmarks showing little movement, there was gradually increase of uplift toward the west, with the maximum value of 20 mm occurred in the westernmost benchmark of the leveling route. It is worth noting that the misfits were small between the leveling and GPS results. Based on the leveling measurements, it does not show any obvious evidence of coseismic slip on the three major faults (i.e., the Central Range, Juisui and Chimei faults) in the area. Instead, it is consistent with the proposed geological interpretation that the 2013 Juisui earthquake resulted from rupturing on a deeper west-dipping structure (Chuang et al., 2014; Lee et al., 2014), potentially the subduction plate interface (Fig. 7b), which did not directly connect to the surface mapped geological faults.

5.2. Reconstruction of the vertical velocity field

To reconstruct the vertical velocity field in the broader regional scale, we incorporated nearby two continuous GPS stations, KNKO (close to Juisui route) and YUL1 (close to Yuli route), from the network of Taiwan-CORS as the reference stations. So that the leveling results for each benchmark can transform into International Terrestrial Reference Frame (ITRF). These two continuous GPS stations have been in operation and provided high-quality observations for more than 15 years since 2002 (Fig. 8) and were estimated for their positioning under the same coordinate system. The vertical velocity of stations in Taiwan-CORS were acquired from the archive database in GPSLAB of Academia Sinica. For both stations KNKO and YUL1, the vertical velocities were estimated to be an identical value of −8.1 mm/yr in 2002–2020 (Fig. 8).

We thus obtained the vertical secular velocity field for the two leveling routes in the middle of the Longitudinal Valley and the Coastal Range (Fig. 9, Table 3). It is interesting and surprising to find that a large portion of the benchmarks shows continuous subsidence, except those in the closer hanging wall of the LVF along the Yuli route. The overall subsidence trend for the two routes during the interseismic periods leads to a few implications. First, at the present day for the long-term time scale across a few earthquake cycles, the study area including the eastern Central Range, Longitudinal Valley and Coastal Range is mostly subsiding at varied rates from −2 to −15 mm/yr. The exception is the hanging wall of the southern LVF (the Chihshang fault) in the Yuli route, where exhibited continuous, rapid uplift. Second, no uplift occurred in the hanging wall of the northern LVF (the Juisui fault) in the Juisui route, although a significant vertical change at a rapid rate of 10 mm/yr across the fault.

Together, it allows us to argue that the overall tectonic context changes from collision in the south (at the level of Yuli route) to subduction (at the level of Juisui route) in the north (Fig. 10). This interpretation is consistent with the seismology-derived plate architecture between the Luzon arc system and Eurasian continental margin (Wu et al., 2009), which proposed the Philippine Sea plate began its NNW-NW subduction near the latitude of Juisui.

6. Conclusions

In this study we presented the results of 9–14 years annual repeated leveling measurements along two E-W trending routes in the middle section of the Longitudinal Valley, the on-land suture of arc-continent collision in eastern Taiwan. We obtained the following conclusions.

(1) In the Juisui route, the leveling results of 2004–2018 indicate that the Central Range fault, the Juisui fault and the Chimei fault were the main responsible for the surface vertical deformation. Continuous tilting upward to the west in the Central Range suggests active slip on the deeper part of the W-dipping Central Range fault that might be coupled with regional folding at the shallow level in the eastern flank of the Central Range. A significant but gradual vertical change at the cumulative rate of 10 mm/yr across the Juisui fault (a segment of LVF) occurred in a width of about 4 km, suggesting the E-dipping thrust fault is active but locked at the upper few kilometers. Across the Chimei fault, a drastic upward pop-up of the turbidite sequence against the volcanic andesitic rocks occurred at a vertical rate of 8 mm/yr along the sub-vertical Chimei fault.

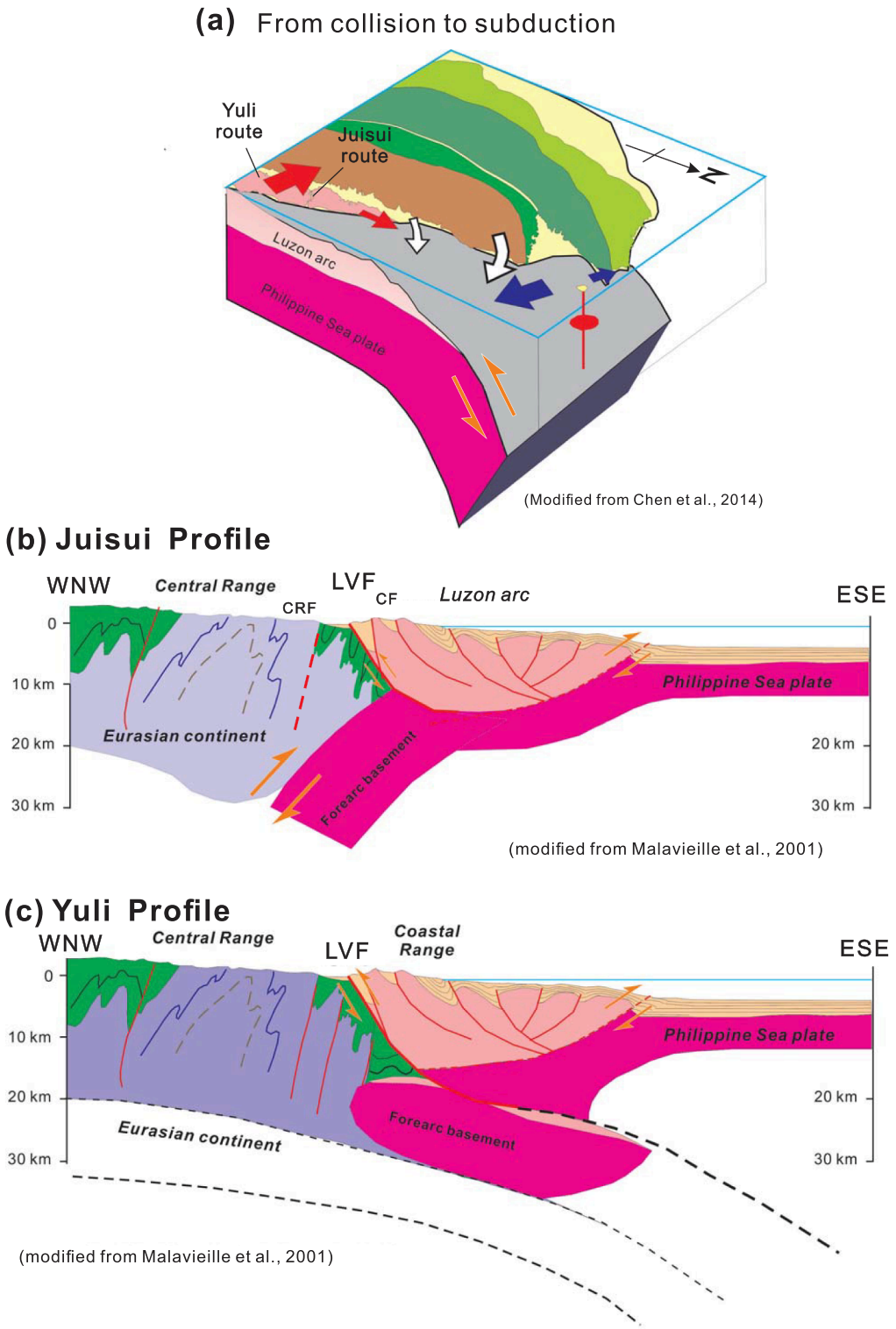

Fig. 10. Architecture of the plate configuration around the convergence between the Luzon arc of the Philippine Sea plate and the Eurasian continental margin. (a) 3-D perspective view of the northern subduction of the Philippine Sea plate in the northeastern Taiwan (after Chen et al., 2014). (b) and (c) E-W geological cross sections in the study area: Juisui profile for the Juisui leveling and Yuli profile for the Yuli leveling (modified from Malavieille et al., 2002). CRF: Central Range fault; LVF: Longitudinal Valley fault; CF: Chimei fault. It appears that the southern part of the LVF (the Yuli profile) is dominated by thrusting with uplift of the Coastal Range, which changes to strike-slip faulting with subsidence/subduction of the Coastal Range in the northern part of the LVF. The Juisui profile is located about the transition area in between.

(2) In the Yuli route, the leveling measurements of 2009–2018 also showed blind deep slip along a W-dipping fault. The Chihshang fault (a segment of the LVF) revealed a creeping behavior without locking in the upper few kilometers at a rapid surface vertical rate of 24–27 mm/yr, more than two times faster than that in the Juisui route. On the other hand, the gradual decrease of vertical changes occurred in the hanging wall of the Chihshang fault with a pair of long-wave anticline and syncline indicate active deformation in the close hanging wall of the fault.
(3) By referencing the results of the Juisui and Yuli routes into global ITRF coordinate system, we find that the middle and southern Longitudinal Valley and Coastal Range is experiencing arc-continental collision with dominated thrusting on the LVF. By contrast, we interpret that the overall tectonic context changed to subduction-driven tectonics toward the north, which started around the latitude of the Juisui route, that was revealed by the overall negative vertical velocity on the surface level.
(4) Our measurements, which were conducted a week before and 2–3 weeks after the 2013 M6.4 Juisui earthquake, showed a co-seismic tilting upward to the west along the Juisui route, from little or no motion near the eastern coastline to the maximum uplift of 20 mm in the Central Range. The results are in agreement with the interpretation of blind slip on the interface of forearc basement of the Luzon arc system in the Philippine Sea plate.

CRediT authorship contribution statement

Horng-Yue Chen: Conceptualization, Data curation, Formal analysis, Investigation, Visualization, Writing - original draft, Writing - review & editing. **Jian-Cheng Lee:** Conceptualization, Formal analysis, Funding acquisition, Investigation, Project administration, Resources, Supervision, Validation, Writing - original draft, Writing - review & editing. **Hsin Tung:** . **Chien-Liang Chen:** Data curation, Investigation. **Hung Kyu Lee:** Data curation, Investigation.

Declaration of Competing Interest

The authors declare that they have no known competing financial interests or personal relationships that could have appeared to influence the work reported in this paper.

Acknowledgements

The authors would like to express their sincere thanks to many colleagues who have devoted their efforts, at different time periods, to the field geodetic surveys for this 15-year-long study. The International GPS Service (IGS) has provided the precise ephemerides for data processing. This research was supported by the Taiwan Earthquake Research Center (TEC) and the Ministry of Science and Technology (MOST) with the grants MOST106-2116-M-001-022 and MOST 107-2116-M-001-001-026-MY3. The paper is a contribution of the Institute of Earth Sciences, Academia Sinica, IESAS2382; and the TEC contribution number for this article is TEC00168.

References

Angelier, J., Chu, H.-T., Lee, J.-C., 1997. Shear concentration in a collision zone: Kinematics of the active Chihshang fault, Longitudinal Valley, eastern Taiwan. Tectonophysics 274, 117–144.
Avouac, J.P., 2015. From geodetic imaging of seismic and aseismic fault slip to dynamic modeling of the seismic cycle. Annu. Rev. Earth Planet. Sci. 43, 233–271.
Biq, C.C., 1972. Dual trench structure in the Taiwan-Luzon region. Proceedings of the Geological Society of China 15, 65–75.
Chang, S.H., Wang, W.H., Lee, J.C., 2009. Modeling surface creep of the Chihshang fault in eastern Taiwan with velocity-strengthening friction. Geophys. J. Int. 176 (2), 601–613. https://doi.org/10.0000/j.1365-246X.2008.03995.x.
Central Geological Survey, 2000. The geological map of Taiwan. Central Geological Survey, Taiwan, ROC, scale 1 (500), 000.
Chen, C.Y., Lee, J.C., Chen, Y.G., Chen, R.F., 2014. Campaigned GPS on Present-day crustal deformation in northernmost Longitudinal Val- ley preliminary results, Hualien Taiwan. Terr. Atmos. Ocean. Sci. 25, 337–357. https://doi.org/10.3319/TAO.2013.12.25.01(TT).
Chen, H.Y., Lee, J.C., Tung, H., Yu, S.B., Hsu, Y.J., Lee, H., 2012. Determination of vertical velocity field of southernmost Longitudinal Valley in eastern Taiwan: a joint analysis of leveling and GPS measurements. Terrestrial Atmospheric and Oceanic Sciences 23 (4), 355–376. https://doi.org/10.3319/TAO.2012.02.29.01.IESAS1653.
Chen, H.Y., Yu, S.B., Kuo, L.C., Liu, C.C., 2006. Coseismic and postseismic displacements of the 10 December 2003 (M_W 6.5) Chengkung, eastern Taiwan, earthquake. Earth Planets Space 58, 5–21.
Chen, H.Y., Hsu, Y.J., Lee, J.C., Yu, S.B., Kuo, L.C., Jiang, Y.L., Liu, C.C., Tsai, C.S., 2009. Coseismic displacements and slip distribution from GPS and leveling observations for the 2006 Peinan Earthquake (Mw 6.1) in southeastern Taiwan. Earth Planets Space 61, 1–20.
Chen, K.H., Yang, M., Huang, Y.T., Ching, K.E., Rau, R.J., 2011. Vertical displacement rate field of Taiwan from geodetic levelling data 2000–2008. Survey Review 43 (321), 296–302.
Chen, W.S., Yen, I.C., Fengler, K.P., Rubin, C.M., Yang, C.C., Yang, H.C., Chang, H.C., Lin, C.W., Lin, W.H., Liu, Y.C., Lin, Y.H., 2007. Late Holocene paleoearthquake activity in the middle part of the Longitudinal Valley fault, eastern Taiwan. Earth Planet. Sci. Lett. 264 (3/4), 420–437.
Chen, W. S. Wang, Y., 1996. Geologic map of Taiwan, scale 1:100,000. Central Geologic Survey, MOEA.
Chu, Y. R., 2016. Magnetic Fabrics Analysis across the Chimei Fault at Chimei Village in the Coastal Range of Eastern Taiwan. Master Thesis, pp. 96, http://rportal.lib.ntnu.edu.tw:80/handle/20.500.12235/101158.
Chuang, R.Y., Johnson, K.M., Kuo, Y.T., Wu, Y.M., Chang, C.H., Kuo, L.C., 2014. Active back thrust in the eastern Taiwan suture revealed by the 2013 Rueisuei earthquake: Evidence for a doubly vergent orogenic wedge? Geophys. Res. Lett. 41, 3464–3470. https://doi.org/10.1002/2014GL060097.
Crespi, J.M., Chan, Y.C., Swaim, M.S., 1996. Synorogenic extension and exhumation of the Taiwan hinterland. Geology 24, 247–250.
Hsu, T.L., 1962. Recent faulting in the Longitudinal Valley of eastern Taiwan. Memoir of the Geological Society of China 1, 95–102.
Hsu, L., Bürgmann, R., 2006. Surface creep along the Longitudinal Valley fault, Taiwan from InSAR measurements. Geophysical Research Letter 33, L06312. https://doi.org/10.1029/2005GL024624.
Huang, Y., Meng, L., Ampuero, J.P., 2012. A dynamic model of the frequency-dependent rupture process of the 2011 Tohoku-Oki earthquake. Earth Planets Space 64 (12), 1061–1066.
Huang, Y., Ampuero, J.P., Kanamori, H., 2014. Slip-weakening models of the 2011 Tohoku-Oki earthquake and constraints on stress drop and fracture energy. Pure applied Geophysics 171, 2555–2568. https://doi.org/10.1007/s00024-013-0718-2.
Kuo, S. T., 2014. Paleostress and fold analysis of the Chimei Fault, Coastal Range, eastern Taiwan. Master Thesis, pp. 117, doi: 10.6342/NTU.2014.00960.
Lee, J.C., Angelier, J., 1993. Localisation des déformations actives et traitements des données géodésiques: l'exemple de la faille de la Vallée Longitudinale, Taïwan. Bulletin de la Societé Géologique de France 164 (4), 533–570.
Lee, J.C., Angelier, J., Chu, H.T., Hu, J.C., Jeng, F.S., Rau, R.J., 2003. Active fault creep variations at Chihshang, Taiwan, revealed by creepmeter monitoring, 1998–2001. J. Geophys. Res. 108 (B11), 2528. https://doi.org/10.1029/2003JB002394.
Lee, J.C., Chu, H.T., Angelier, J., Hu, J.C., Chen, H.Y., Yu, S.B., 2006. Quantitative analysis of co-seismic surface faulting and post-seismic creep accompanying the 2003, Mw=6.5, Chengkung earthquake in eastern Taiwan. J. Geophys. Res. 111, B02405. https://doi.org/10.1029/2005JB003612.
Lee, C., Yu, S.B., 1985. Precision of distance measurements for observing horizontal crustal deformation in Taiwan. Bulletin of the Institute of Earth Sciences, Academia Sinica 5, 161–174.
Lee, S. J., Huang, H. H., Shyu, J. Bruce H., Lin, T. C., Yeh, T. Y., 2014. Numerical earthquake model of the 31 October 2013 Ruisui, Taiwan, Earthquake: Source rupture process and seismic wave propagation, Journal of Asian Earth Sciences, 96, 374-385, doi:10.1016/j.jseaes. 2014.09.020.
Liu, C.C., Yu, S.B., 1990. Vertical crustal movement in eastern Taiwan and its tectonic implications. Tectonophysics 183, 111–119.
Malavieille, J., Lallemand, S. E., Dominguez, S., Deschamps, A., Lu, C. Y., Liu, C. S., Schnuerle, P., Angelier, J., Collot, J. Y., Deffontaines, B., Fournier, Hsu, M. S. K., Formal, J. P., Liu, L. S. Y., Sibuet, J. C., Thareau, N., Wang, F., the ACT (Active Collision in Taiwan) Scientific Crew, 2002. Arc-continent collision in Taiwan: New marine observations and tectonic evolution, In: Timothy B. Byrne, C. S. Liu (Eds.), Geology and geophysics of an arc-continent collision, Taiwan 358, pp. 187-211, doi: 10.1130/0-8137-2358-2.187.
Murase, M., Matta, N., Lin, C.H., Chen, W.S., Koizumi, N., 2013. An episodic creep-slip event detected by precise levelling surveys in the central part of the Longitudinal Valley Fault, eastern Taiwan, in 2011–2012. Tectonophysics 608, 904–913.
Peyret, M., Dominguez, S., Cattin, R., Champenois, J., Leroy, M., Zajac, A., 2011. Present-day interseismic surface deformation along the Longitudinal Valley, eastern Taiwan, from a PS-InSAR analysis of the ERS satellite archives. J. Geophys. Res. 116, B03402. https://doi.org/10.1029/2010JB007898.
Schomaker. M.C., Berry, R.M., 1981. Geodetic leveling, in NOAA Manual NOS NGS 3. National Oceanic and Atmospheric Administration, Rockville, Maryland. 209 pp.
Shyu, J. B. H., Sieh, H, K., Chen, Y. G., Liu, C. S., 2005. Neotectonic architecture of Taiwan and its implications for future large earthquakes. Journal of Geophysical Research 110, B08402. doi:10.1029/2004JB003251.

Thatcher, W., Rundle, J., 1979. A model for the earthquake cycle in underthrust zones. J. Geophys. Res. 84 (B10), 5540–5556.

Thomas, M.Y., Avouac, J.P., Champenois, J., Lee, J.C., Kuo, L.C., 2014. Spatiotemporal evolution of seismic and aseismic slip on the longitudinal Valley Fault. Taiwan. Journal of Geophysical Research 119, 5114–5139. https://doi.org/10.1002/2013JB010603.

Thomas, M.Y., Avouac, J.P., Lapusta, N., 2017. Rate-and-state friction properties of the Longitudinal Valley Fault from kinematic and dynamic modeling of seismic and aseismic slip. J. Geophys. Res. 122, 3115–3137. https://doi.org/10.1002/2016JB013615.

Vergne, J., Cattin, R., Avouac, J.P., 2001. On the use of dislocations to model interseismic strain and stress build-up at intracontinental thrust faults. Geophys. J. Int. 147, 155–162.

Wu, F.T., Liang, W.T., Lee, J.C., Benz, H., Villasenor, A., 2009. A model for the termination of the Ryukyu subduction zone against Taiwan: A junction of collision, subduction/separation, and subduction boundaries. J. Geophys. Res. 114, B07404. https://doi.org/10.1029/2008JB005950.

Yen, J.Y., Lu, C.H., Chang, C.P., Hooper, A., Chang, Y.H., Liang, W.T., Chang, T.Y., Lin, M.S., Chen, K.S., 2011. Investigating the active deformation in the northern Longitudinal Valley and Hualien City of eastern Taiwan by using Persistent Scatter and Small-baseline SAR Interferometry. Terrestrial Atmospheric and Oceanic Sciences 22 (3), 291–304. https://doi.org/10.3319/TAO.2010.10.25.01(TT).

Yu, S.B., Lee, C.C., 1986. Geodetic measurements of horizontal crustal deformation in eastern Taiwan. Tectonophysics 125, 73–85.

Yu, S.B., Chen, H.Y., 1994. Global Positioning System measurements of crustal deformation in the Taiwan arc-continent collision zone. Terrestrial Atmospheric and Oceanic Sciences 5 (4), 477–498.

Yu, S.B., Yu, G.K., Kuo, L.C., Lee, C., 1992. Crustal deformation in the southern Longitudinal Valley area, eastern Taiwan. J. Geol. Soc. China 35 (3), 219–230.

Yu, S.B., Kuo, L.C., 2001. Present-day crustal motion along the Longitudinal Valley Fault, eastern Taiwan. Tectonophysics 333, 199–217.